Journal of the European Ceramic Society **19** (1999) 2667–2675

PII: S0955-2219(99)00040-0
0955-2219/99/$ - see front matter

New Evidence for Rhombohedral Symmetry in the Relaxor Ferroelectric $Pb(Mg_{1/3}Nb_{2/3})O_3$

Noel W. Thomas,[a]* Sergey A. Ivanov,[b]† Supon Ananta,[a] Roland Tellgren[c]‡ and Häkan Rundlof[c]

[a]Department of Materials, University of Leeds, Leeds LS2 9JT, UK
[b]Karpov Institute of Physical Chemistry, Moscow, Russia
[c]Inorganic Chemistry, Ångstrom Laboratory, Uppsala University, Uppsala, Sweden

(Received 12 August 1998; accepted 6 February 1999)

Abstract

Neutron diffraction data have been collected from powders of lead magnesium niobate (PMN) at 300 and 10 K, following their synthesis in an optimised two-step reaction. Subsequent Rietveld refinement indicates that macroscopic rhombohedral symmetry is obtained at both temperatures. Moreover, the existence of a polar structure at room temperature has been independently confirmed by second harmonic generation measurements. The derived crystal structures indicate R3m *and* R3c *symmetry at 300 and 10 K, respectively. The significance of these results for an understanding of the mechanism of relaxor ferroelectricity in PMN is discussed.* © *1999 Elsevier Science Limited. All rights reserved*

Keywords: neutron diffraction, crystal structure, PMN, ferroelectric properties, niobates.

1 Introduction

Lead magnesium niobate, $Pb(Mg_{0.33}Nb_{0.67})O_3$ (PMN), belongs to a class of complex $Pb(B'B'')O_3$ perovskites known as ferroelectric relaxors. First discovered in 1958,[1] this compound exhibits both a diffuse maximum in the variation of relative permittivity with temperature and a strong frequency dispersion, with $T(\varepsilon_{r,\max})$ lying in the range 253–263 K at 100 Hz. Furthermore, X-ray, neutron, electron diffraction and HRTEM studies of pure PMN ceramics have revealed compositional and structural heterogeneities.[2,3] The diffuse scattering observed in X-ray and neutron diffraction patterns may be assigned to the existence of polar regions dispersed in the main cubic matrix,[4] which result from local correlated atomic displacements. It has also been proposed that rhombohedral nanodomains, in which the Mg^{2+} and Nb^{5+} cations are 1:1 ordered in the B site of the perovskite structure[5,6] nucleate, on cooling, at about 600 K.[7] Subsequent growth to sizes of the order of 100 Å has also been observed at temperatures below 160 K.[8]

Many attempts have been made to explain the typical relaxor dielectric response of PMN.[9–14] The heterogeneous microregion model,[9] which is generally accepted, regards the diffuse phase transition as fundamentally due to local compositional fluctuations associated with B-site cation disorder, these resulting in a distribution of Curie temperatures. Further insight into the nature of relaxor dielectric behaviour has been provided by the suggestion that the polar microregions are analogous to spin clusters in superparamagnetic materials.[9] Moreover, a direct connection between localized B-site cation ordering and relaxor properties has also been proposed.[10]

The symmetries of the different phases of PMN, despite the generally accepted cubic symmetry at room temperature, are still under debate,[12–14] with the crystal chemistry now regarded as more complicated than formerly anticipated.[15–20] In particular, ambiguity over the symmetry of PMN at room temperature persists. Whereas this is generally regarded as cubic,[1–3] speculation over lower symmetry alternatives remains, with orthorhombic symmetry proposed in a recent structural refinement.[16]

That straightforward cubic symmetry should not prevail in PMN at room temperature can be deduced from general considerations, without recourse to the detailed interpretation of experimental results (as carried out here, for example). First, and foremost, this temperature lies within the

*To whom correspondence should be addressed present address: WBB Technology, Watts Blake Bearne & Co plc, Park House, Courtenay Park, Newton Abbot, Devon TQ12 4PS, UK. Fax: +44-(0)1626-322386; e-mail: nthomas@wbb.co.uk
†E-mail: ivan@cc.nifhi.ac.rv
‡E-mail: rte@studsvik.uu.se

'Curie range', over which a diffuse maximum in the relative permittivity is observed. It would therefore be illogical to suppose that, at room temperature, all the material would be in a paraelectric state with cubic symmetry. There are also indications that a tendency towards rhombohedral symmetry exists (rather than orthorhombic[16]). For example, there is widespread acceptance that the solid solution system PMN–PT has rhombohedral symmetry for PT concentrations of up to 30 to 32·5 mole per cent,[21] although the symmetry for low levels of titanium-substitution remains unclear. This macroscopic polar symmetry can be regarded as a consequence of the Ti^{4+} ions forming strong dipolar TiO_6^{8-} octahedral units, along with the need to accommodate relatively large Mg^{2+} ions through octahedral distortions allowed in rhombohedral symmetry. The importance of these distortions, which are allowed in rhombohedral, but not in orthorhombic symmetry, has also been demonstrated in the PMN–PZ (i.e. $Pb(Mg_{1/3}Nb_{2/3})O_3$–$PbZrO_3$) system, where progressive substitution of the relatively large Zr^{4+} ion is found to increase the temperature of maximum permittivity, implying the stabilisation of a polar phase.[22] Thus it is reasonable to ask whether rhombohedral symmetry should not also exist in the parent composition, PMN, at room temperature. A secondary question is whether this symmetry can be regarded as macroscopic, i.e. extending throughout all parts of the crystallites, or whether it is confined to polar clusters within a matrix of cubic symmetry.

The present work utilises the techniques of neutron powder diffraction/Rietveld refinement and second harmonic generation to address these questions. In forming a conclusion over whether rhombohedral or cubic symmetry is adopted, the argument will not depend critically on whether the three cell parameters α, β, γ obtained from the refinement deviate from 90°, since it is possible to have rhombohedral symmetry with interaxial angles which are *equal* to 90°, to within experimental error. Attention will be focused instead on the positional parameters of the oxygen ions, and the extent to which these indicate $(Mg,Nb)O_6$ octahedral distortions, which can occur in rhombohedral symmetry, but not in cubic. It is the importance of determining these oxygen ion positions which dictates the use of powder diffraction by neutrons rather than X-rays. In general, the latter are unable to yield precise information about order parameters of perovskite phase transitions, these being related mainly to tilting and distortion of the $(Mg,Nb)O_6$ octahedra.

Here a neutron powder diffraction study of PMN at 300 and 10 K has been carried out. Whereas the results at 300 K are clearly of more direct interest, an examination of the structural parameters obtained at 10 K is relevant to the general problem of identifying the true symmetry of PMN. Since the tendency towards the formation of polar phases is increased upon cooling, a clear, unambiguous result of rhombohedral symmetry at 10 K would lend strong support to the possibility of this symmetry being maintained at room temperature.

2 Method

Single-phase PMN powders were prepared by an optimised two-step calcination method involving columbite-like $MgNb_2O_6$ intermediates.[23] Neutron powder diffraction (NPD) data were collected at the Swedish Research Reactor R2 in Studsvik, by means of a Huber two-circle diffractometer with an array of 35 ^{3}He detectors. The monochromator system used two parallel copper crystals in (220)-mode, giving rise to a wavelength of 1·470 Å. The neutron flux at the sample position was approximately 10^6 neutrons $cm^{-2}\,s^{-1}$. Data were collected at 300 and 10 K from powdered samples of PMN (approximately 5 g) loaded into a vanadium container, with detector intensities statistically analysed and summed. Corrections for absorption effects were subsequently carried out in the Rietveld refinements, utilising the empirical value $\mu R = 0{\cdot}0645\,cm^{-1}$. The step-scan covered the 2θ range 4–140° with step-size 0·05°.

Diffraction datasets were refined by the Rietveld method using FULLPROF software,[24] with neutron scattering lengths as follows: Pb: 9·40; Mg: 5·38; Nb: 7·05; O: 5·81 fm. Diffraction peaks were quantified by a pseudo-Voigt function, with a peak asymmetry correction applied at angles below 35° 2θ. The background was described by a six parameter polynomial. Each structural model was refined to convergence, with the best result selected on the basis of agreement factors and stability of the refinement.

The Second Harmonic Generation (SHG) technique (Nd:YAG laser, reflection geometry, quartz standard) was used as a sensitive and reliable method for establishing the presence or absence of a centre of symmetry at room temperature. Powders of particle size 4–5 μm were prepared for this purpose.

3 Results

The room-temperature X-ray diffraction pattern of PMN powder could be readily identified as due to a perovskite-related phase with a pseudo-cubic cell

of length ca 404 pm (Fig. 1). Inspection of the neutron powder diffraction pattern provided no evidence for ordering of Mg and Nb, which would result in a doubling of the unit cell. Owing to the absence of a (111) pseudo-cubic peak (referred to doubled axes), models based on ordered B-cation distributions were not considered further.

Rietveld refinements of the neutron diffraction data indicated a single phase with nominal cationic and anionic stoichiometry (to within 1%) (Fig. 2). The room temperature NPD data for PMN were initially refined in s.g. Pm3m with idealized coordinates. The final agreement factors obtained in the refinement were $R_p = 5{\cdot}10$, $R_{wp} = 6{\cdot}74$, $R_{exp} = 3{\cdot}87$,

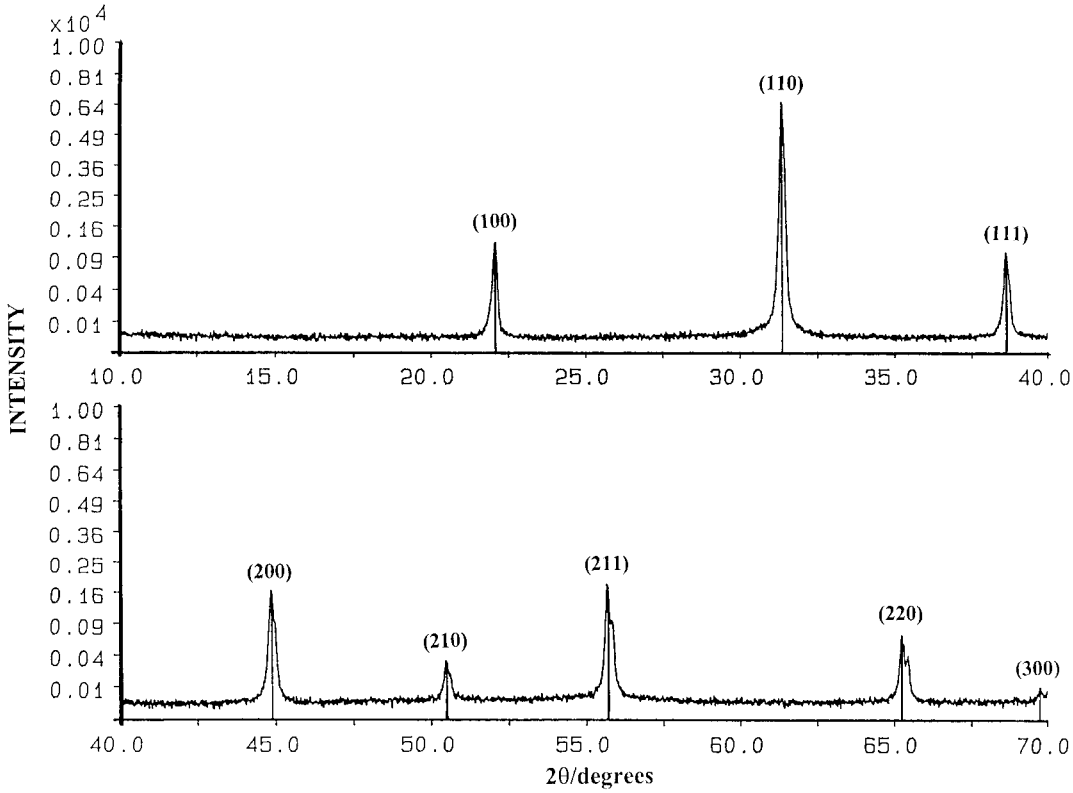

Fig. 1. XRD pattern of the PMN powder.

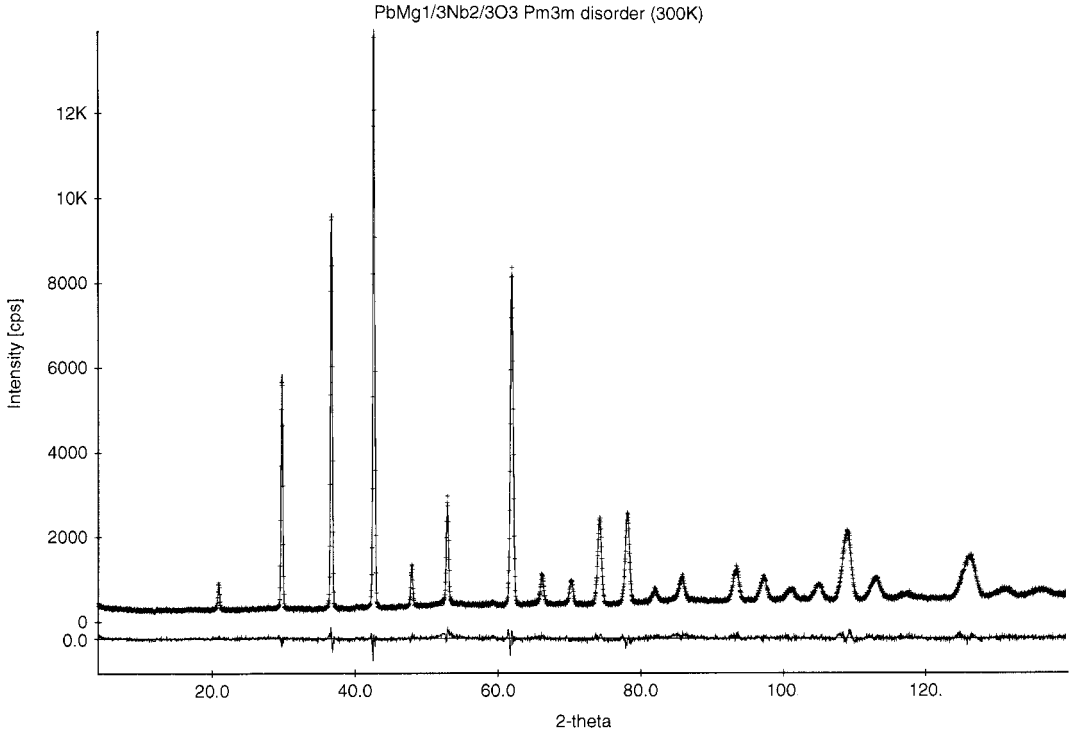

Fig. 2. Rietveld profile-fitting for a disordered model for PMN at 300 K.

$R_B = 6{\cdot}04$, together with a large, but stable value of the B_{iso} thermal parameter of the Pb cation, 3.98(6) Å^2. This indicates significant average displacements of Pb ions from their equilibrium positions. Similarly large B_{iso}-values obtained for other lead-containing perovskites [e.g. $PbTiO_3$, $PbZrO_3$, $Pb(Co,W)O_3$, $Pb(Sc,Nb)O_3$ and $Pb(Fe,Ta)O_3$] have been interpreted as due to a lack of long range order or to the presence of either static disorder/short range order.[25–27]

Five structural models were subsequently tested, with the Pb cation distributed over the 6 (*x*00), 8 (*xxx*), 12 (*xxo*), 24 (*xxz*) or 48 (*xyz*) equivalent positions around the origin of the cubic cell. All models with Pb on (*x*00), (*xxz*) or (*xyz*) sites gave oscillatory or ill-conditioned refinements, and failed to converge. By comparison, structural models with the lead ion occupying positions (*xxx*) and (*xx*0) refined successfully, leading both to small shifts of the cation from the origin and to a significant reduction in the B_{iso} thermal parameter. However, correlations between the displacements and thermal parameters of lead ions were observed. Although reductions in the R-factors were also obtained, these improvements were regarded as physically insignificant, since, in general, any increase in the number of parameters in the least squares fitting would give rise to reductions of this kind. A similar procedure was applied to the Mg/Nb and O ions, before finally refining all atomic shifts simultaneously. The results of this refinement are given in Table 1.

A more detailed analysis of the powder pattern indicated some additional features which were incompatible with cubic symmetry. Profile fitting of the pseudo-cubic (222) reflection showed a unexpected, clearly recognizable shoulder (Fig. 3), suggesting that a decomposition of the initial profile into two rhombohedral peaks, $(222)_R$ and $(-222)_R$ would be appropriate. Further support for this option was provided by the SHG tests, where the $I(2\omega):I(2\omega)_{SiO_2}$ ratio obtained was 3·9(1). Since the threshold value of this ratio between centro- and non-centrosymmetric crystals is 0·01, a strong indication was thereby given of the lack of a centre of symmetry.

The NPD pattern of PMN at 300 K was refined in space groups *R3m* and *R3c* (referred to hexagonal axes). Mg and Nb were assumed to occupy the B sites randomly in a 1:2 ratio. No extra peaks or additional splitting of the main reflections were observed. The refined atomic positions, isotropic temperature factors, occupancy factors and agreement indices for PMN at 300 K are given in Table 2. It is to be noted that the *R*-factors for the *R3c* model are slightly greater than for *R3m*. The models used in the refinement assumed full occupancy of all sites. Moreover, attempts to refine site occupancy factors did not lead to significantly improved agreement indices. The quality of the fit for the *R3m* model is shown in Fig. 4.

For all the models investigated, a comparison of observed and calculated diffraction profiles indicated that good fits were consistently obtained for reflections with (hkl) indices of the same parity. Conversely, some discrepancies connected with widening of peak-bases (diffuse scattering) were observed for peaks with indices with different parities (particularly with two odd indices), as has been observed previously.[11]

In accordance with a structural model proposed earlier,[16] attempts were also made to refine a structural model in space groups *Pnma* and *Cmcm* from our data. However, these refinements did not lead to polar structures, this being at variance with SHG results. Additional support for rhombohedral symmetry in PMN has been provided by precision Raman spectra.[28,29] Experimental evidence for this symmetry has also been gained from poled PMN and 0·9 (PMN)–0·1 (PT) ceramics.[30–33]

Table 1. Refined cubic structural parameters for (*xx0*) and (*xxx*) displacements of Pb ions at 300 K

Space group $Pm\bar{3}m$, lattice parameter: 4·0385 (1) Å $R_p = 5{\cdot}06$, $R_{wp} = 6{\cdot}66$, $R_{exp} = 3{\cdot}87$, $R_B = 5{\cdot}79$

Atom	*x*	*y*	*z*	*B* (Å^2)
Pb	0·0540 (26)	0·0540 (26)	0	1·12 (4)
Mg/Nb	0·4921 (19)	0·4921 (19)	0·4921 (19)	0·18 (2)
O	0·5264 (23)	0·5264 (23)	−0·0079 (27)	1·49 (5)

Space group $Pm\bar{3}m$, lattice parameter: 4·0385 (1) Å $R_p = 4{\cdot}92$, $R_{wp} = 6{\cdot}48$, $R_{exp} = 3{\cdot}87$, $R_B = 5{\cdot}51$

Atom	*x*	*y*	*z*	*B* (Å^2)
Pb	0·0451 (28)	0·0451 (28)	0·0451 (28)	0·96 (3)
Mg/Nb	0·4891 (16)	0·4891 (16)	0·4891 (16)	0·22 (2)
O	0·5303 (21)	0·5303 (21)	−0·0053 (29)	1·36 (4)

Table 2. Alternative rhombohedral structures of PMN at 300 K

Space group *R3m*. Cell parameters (Å): $a = 5{\cdot}7104$ (1), $c = 6{\cdot}9960$ (1) $R_p = 4{\cdot}60$, $R_{wp} = 6{\cdot}13$, $R_{exp} = 3{\cdot}86$, $R_B = 4{\cdot}57$

Atom	*x*	*y*	*z*	*B* (Å^2)
Pb	0	0	0	2·26 (8)
Mg/Nb	0	0	0·4920 (18)	0·61 (3)
O	0·1721 (11)	−0·1721 (11)	0·3394 (14)	1·44 (5)

Space group *R3c*. Cell parameters: $a = 5{\cdot}7103$ (1) Å, $c = 13{\cdot}9956$ (2) Å $R_p = 4{\cdot}84$, $R_{wp} = 6{\cdot}41$, $R_{exp} = 3{\cdot}86$, $R_B = 5{\cdot}35$

Atom	*x*	*y*	*z*	*B* (Å^2)
Pb	0·3333	0·6667	0·4170 (13)	2·31 (6)
Mg/Nb	0	0	1/2	0·56 (2)
O	0·1758 (16)	0·3416 (14)	0·5784 (11)	1·46 (4)

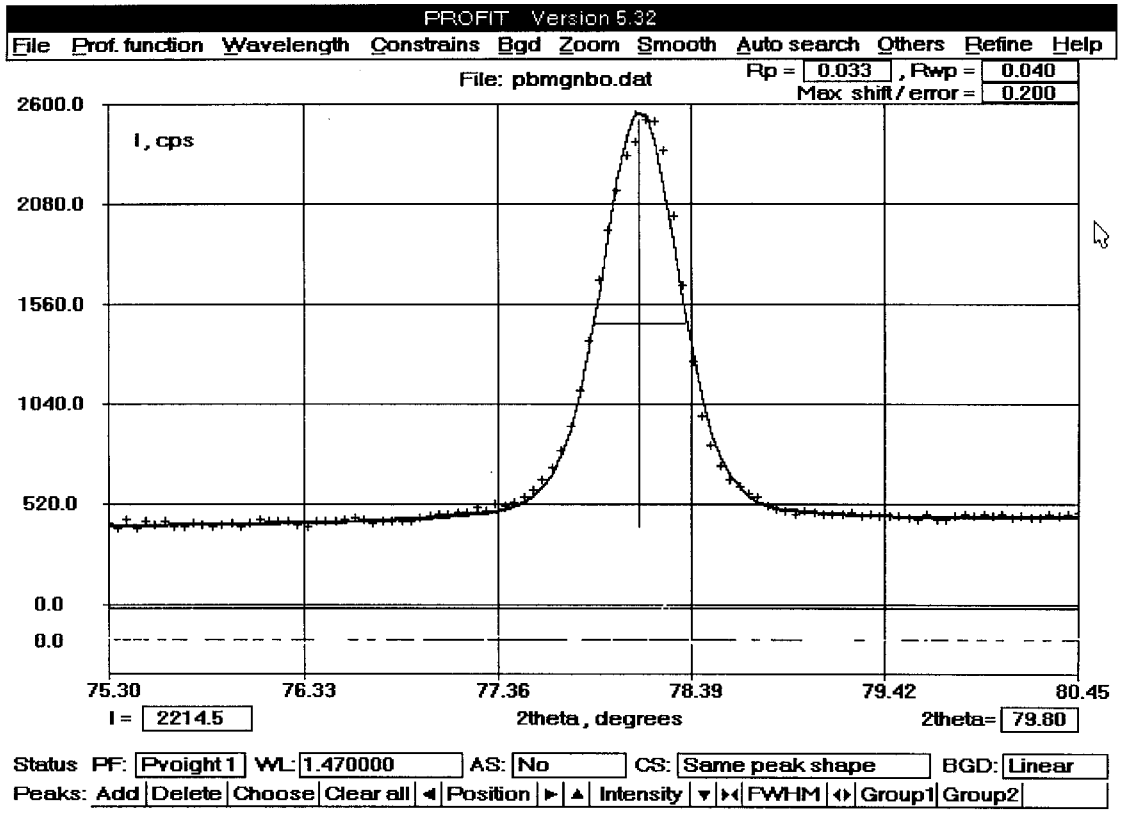

(a)

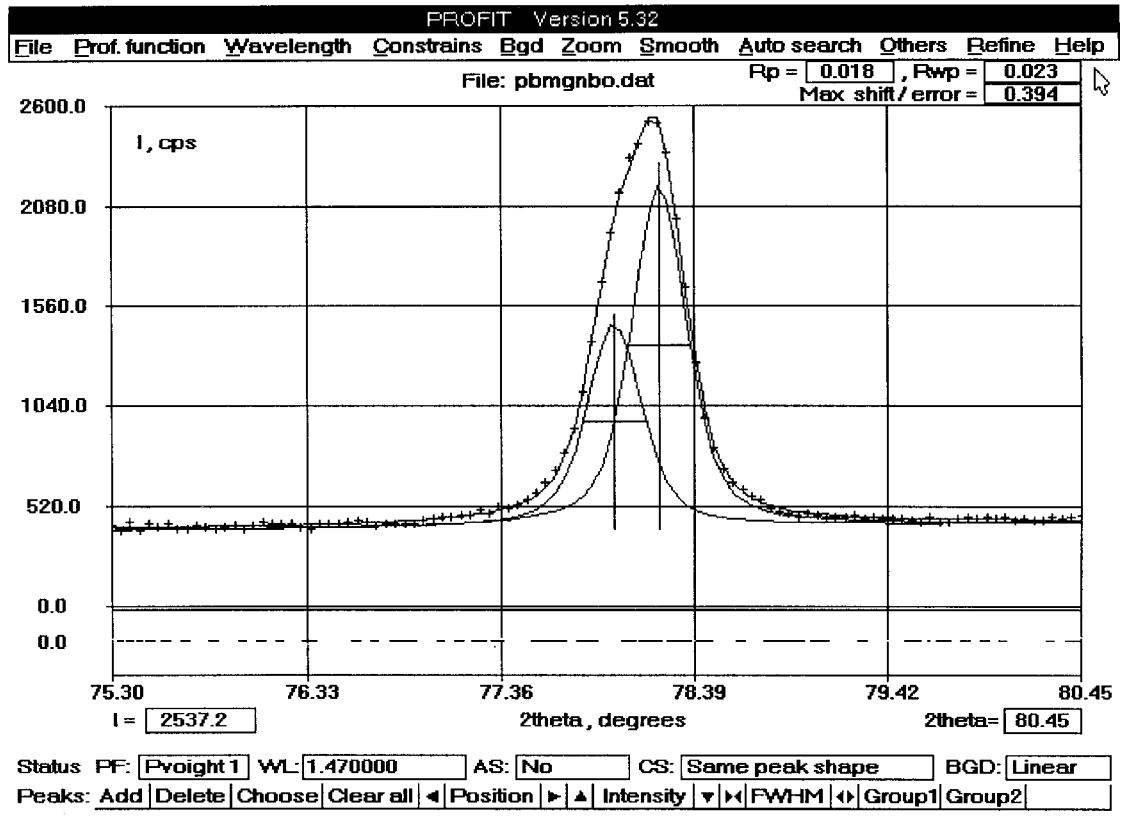

(b)

Fig. 3. Profile fitting of the pseudo-cubic (222) reflection (a) by a single pseudo-Voigt profile; and (b) by two pseudo-Voigt profiles (as would be necessary for rhombohedral symmetry). The improvement in the fitting with two profiles is quantified by the parameter $R_p = 100\ \Sigma \mid y_{oi} - y_{ci} \mid / \Sigma \mid y_{oi} \mid$, where y_{oi} and y_{ci} refer to observed and calculated intensities at experimental points i, which are marked by crosses. R_p is equal to 0·033 cps for (a) and 0·018 for (b).

Having established that rhombohedral symmetry was appropriate at 300 K, refinement into space groups *R3m* and *R3c* was carried out from the low temperature (i.e. 10 K) neutron data, with the fits shown in Figs 5 and 6. The calculated atomic coordinates and isotropic temperature factors are listed in Table 3.

4 Discussion

Three essential issues arise from the results: (i) whether rhombohedral or cubic symmetry applies at 300 K; (ii) given the evidence in favour of rhombohedral symmetry, which of *R3m* or *R3c* symmetry is appropriate at both 300 and 10 K; and

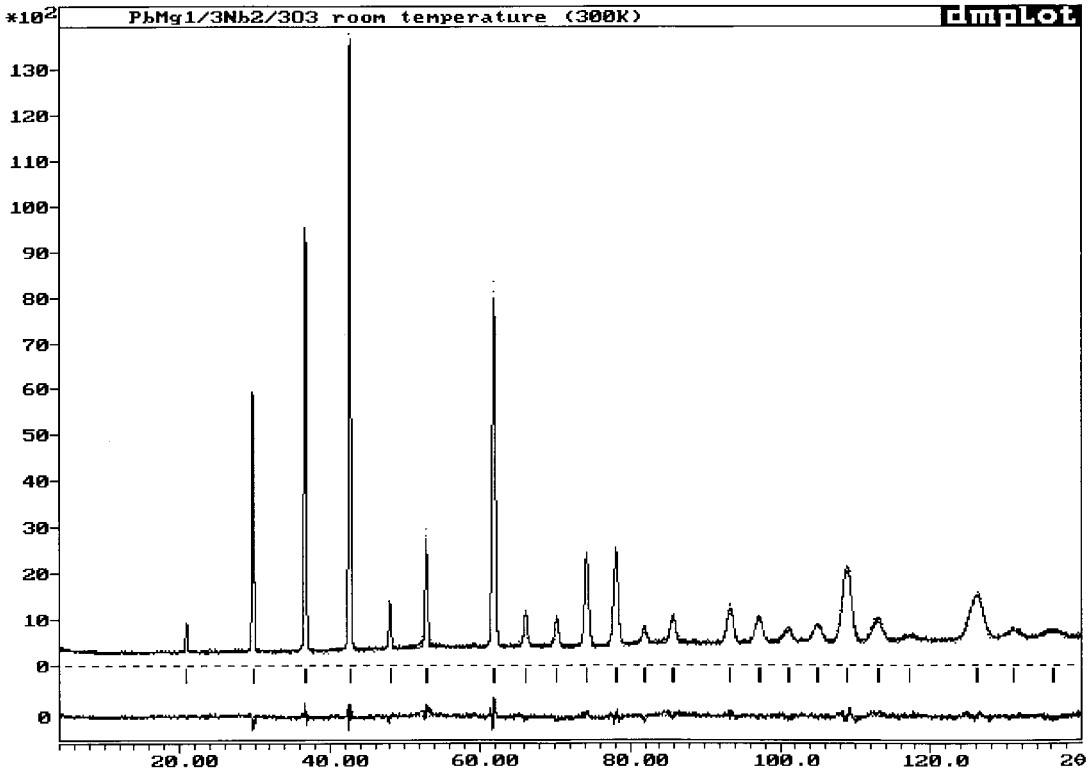

Fig. 4. Rietveld profile-fitting for the rhombohedral *R3m* structure at 300 K.

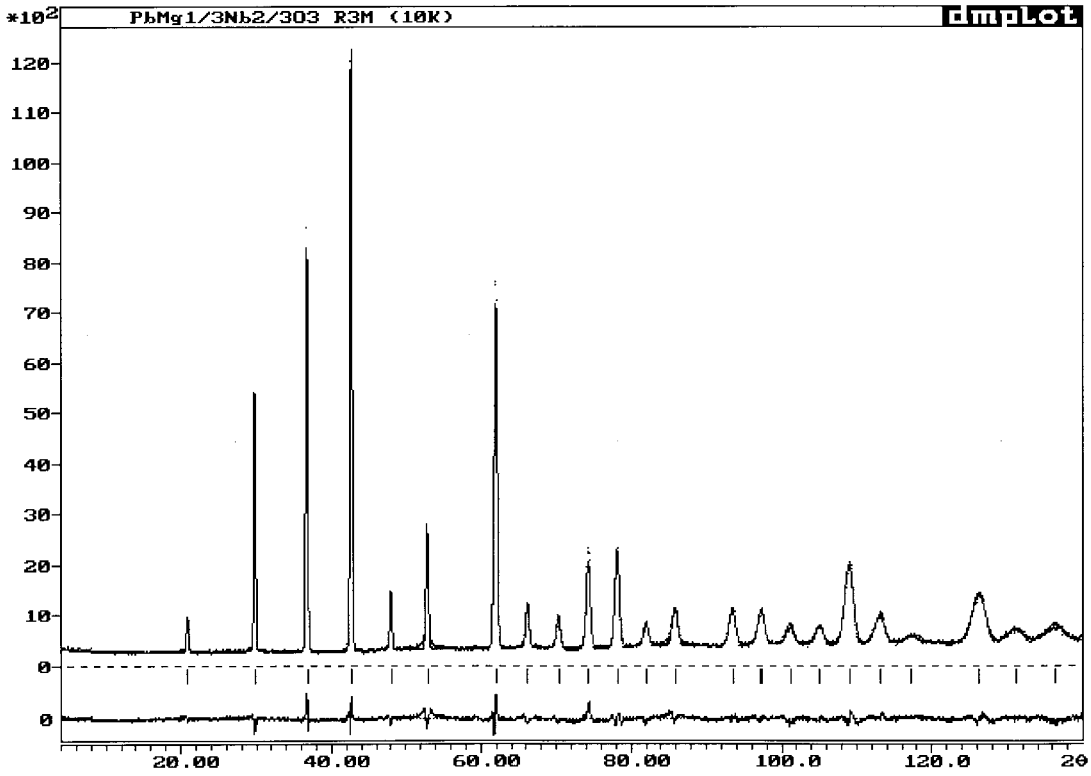

Fig. 5. Rietveld profile-fitting for the rhombohedral *R3m* structure at 10 K.

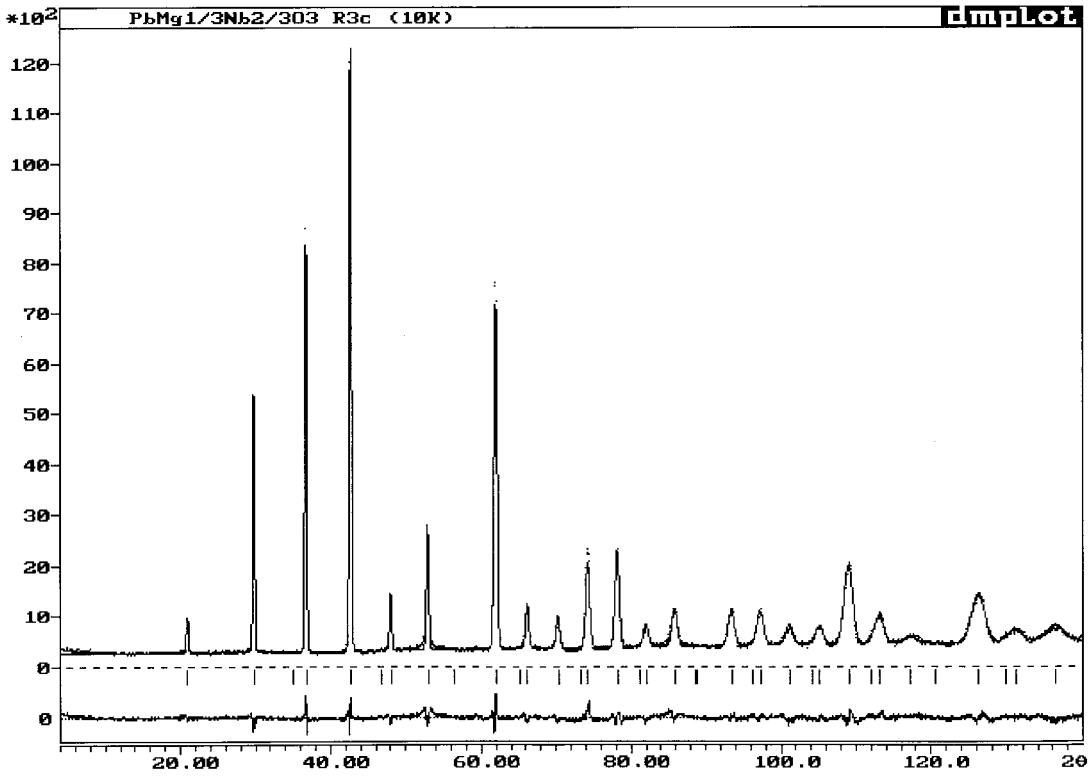

Fig. 6. Rietveld profile-fitting for the rhombohedral *R3c* structure at 10 K.

(iii) the nature of the coordination of the lead ion in PMN.

As has been set out in the Introduction, the positional parameters of the oxygen ions are of overriding importance in dealing with the first question. If the symmetry were cubic, the oxygen parameters with hexagonal axes would be $x=0{\cdot}1667$; $y=-0{\cdot}1667$; $z=0{\cdot}3333$, where the origin of the cell is defined by the Pb-ion position. It is seen from our results in Table 2 that the oxygen parameters deviate from these values by $(\Delta x, \Delta y, \Delta z)=(0{\cdot}0054, -0{\cdot}0054, 0{\cdot}0061)$, all these being at least 4 times greater than the respective standard deviations. Thus there is strong evidence for the symmetry being rhombohedral. Additional evidence is provided by the Mg/Nb z-coordinate, which, at $z=0.4920$, also deviates from the cubic value of 0·5000 by more than four standard deviations. Furthermore, the cell parameters obtained suggest that rhombohedral symmetry is appropriate, since the c/a-ratio, at 6·9960/5·7104 (=1·22513) deviates from the ratio for cubic symmetry of $\sqrt{3}/\sqrt{2}$ (=1·22474). This still holds for values of c/a at one standard deviation away from the quoted values, i.e. $c_{1\sigma}/a_{1\sigma}=6{\cdot}9959/5{\cdot}7105=1{\cdot}22509$. Finally, the SHG results support polar symmetry rather than an unpolar, cubic alternative.

Table 3. Alternative rhombohedral structures of PMN at 10 K

Space group: *R3m*, $a=5{\cdot}7069$ (1) Å, $c=6{\cdot}9911$ (1) Å, $R_p=5{\cdot}42$, $R_{wp}=7{\cdot}24$, $R_{exp}=4{\cdot}05$, $R_B=5{\cdot}91$

Atom	*x*	*y*	*z*	*B* (Å^2)
Pb	0·0000	0·0000	0·0000	2·08 (3)
Mg/Nb	0	0	0·4951 (17)	0·14 (2)
O	0·1726 (12)	−0·1726 (12)	0·3506 (18)	1·17 (3)

Space group: *R3c*, $a=5{\cdot}7068$ (1) Å, $c=13{\cdot}9824$ (1) Å, $R_p=5{\cdot}46$, $R_{wp}=7{\cdot}30$, $R_{exp}=4{\cdot}05$, $R_B=5{\cdot}44$

Atom	*x*	*y*	*z*	*B* (Å^2)
Pb	0·3333	0·6667	0·415 (13)	2·27 (4)
Mg/Nb	0	0	1/2	0·14 (2)
O	0·1772 (12)	0·3453 (11)	0·5728 (16)	1·01 (3)

In connection with the second question, it is appropriate to compare the high- and low-temperature structures in both symmetries in terms of the crystal-chemical framework proposed earlier for rhombohedral perovskites.[34–36] As discussed recently,[37] *R3c* structures have six degrees of freedom, compared to five in *R3m*. The extra structural parameter in *R3c* allows there to be a non-zero octahedral tilt angle, ω (Table 4). The *R3m* structure is the preferable model for the room temperature diffraction data, since lower R_p and R_{wp} factors are obtained, despite there being one fewer parameter against which the refinement can be carried out. Conversely, the *R3c* structure appears to be more appropriate at 10 K: whereas R_p and R_{wp} are practically identical, R_B is smaller for *R3c* than for *R3m*.

Although caution should be exercised is basing the argument solely on a consideration of *R*-factors, particularly since *R3c* has one more parameter in the refinement, a crystal-chemical analysis of the four structural solutions is also supportive of *R3c* symmetry at 10 K. A consideration of Table 4 reveals that a change from *R3m* to *R3c* symmetry

Table 4. Crystal structural parameters of the four rhombohedral structures of PMN, utilising the following parameters: V_{Pb}:PbO_{12} polyhedral volume; $V_{Mg/Nb}$:MgO_6 polyhedral volume; As: octahedral distortion perendicular to trigonal axis; n: octahedral elongation parallel to trigonal axis; Δz_{Pb}, $\Delta z_{Mg/Nb}$, displacements of Pb and Mg/Nb ions parallel to trigonal axis

Structure	V_{Pb} *(Å³)*	$V_{Mg/Nb}$ *(Å³)*	$V_{Pb}/V_{Mg/Nb}$	Δs *(pm)*	η	Δz_{Pb} *(pm)*	$\Delta z_{Mg/Nb}$ *(pm)*	ω *(°)*
R3m (300 K)	54·8796	10·9753	5	9·31	1·00031	4·24	9·84	0
R3m (10 K)	54·7740	10·9548	5	10·16	1·00022	12·10	15·53	0
R3c (300 K)	54·8885	10·9817	4·9982	7·08	1·00046	7·36	6·91	0·9929
R3c (10 K)	54·7701	10·9572	4·9985	10·24	1·00016	12·40	14·73	0·9042

upon cooling from 300 to 10 K permits a reduction in the PbO_{12} polyhedral volume (as is normally the case on cooling), whilst the BO_6 polyhedral volume ($B \equiv (Mg_{1/3}Nb_{2/3})$ can remain approximately constant. This is not possible in *R3m*, where the octahedral tilt angle of zero constrains the PbO_{12}:BO_6 polyhedral volume-ratio to be fixed at 5.

It is also seen in Table 4 that the values of four of the structural parameters, i.e. Δs, η, Δz_{Pb} and $\Delta z_{Mg/Nb}$, are relatively invariant between the *R3m* and *R3c* solutions at a given temperature. This observation provides solid support for the existence of rhombohedral symmetry at both temperatures, with increases in both octahedral distortion and cationic displacements occurring on cooling.

A discussion of the third issue, i.e. the coordination of the lead ion in PMN is prompted by the consistently large isotropic temperature factors, B_{iso}, obtained for the lead ions in all rhombohedral structures (Table 2 and Table 3). However, a literal interpretation, that the lead ions have large vibrational amplitudes is unlikely to be the underlying cause of these results. It is more likely that there is positional disorder of the lead ions, such that the vector sum of all components of the lead ion displacements perpendicular to the trigonal axis is zero. In this connection, it is pertinent to note that recent neutron diffraction studies of rhombohedral PZT ($PbZr_{1-x}Ti_xO_3$; $0{\cdot}08 \leq x \leq 0{\cdot}33$) have also highlighted difficulties in representing the positions of the lead ion by a straightforward displacement parallel to the trigonal axis.[38] In terms of pseudocubic axes, more satisfactory Rietveld refinements were obtained by combining $[111]_p$ shifts with displacements averaged over $[100]_p$, $[010]_p$ and $[001]_p$ directions. Such displacements would allow the lead ions to be coordinated more closely with three symmetrically equivalent triangular faces of their O_{12} coordination polyhedron, such a geometry being consistent with the generally perceived covalent bonding requirements of the lead ion. In qualitative terms, such a geometry would permit optimised directional bonding consistent with sp^3 hybridisation, whilst at the same time permitting the $6s^2$ lone pair on the lead ion to be directed away from the repulsive oxygen ions constituting the coordination polyhedron.

Work is currently in progress on these issues, since they will have a direct bearing on the underlying mechanism of ferroelectricity in lead-based relaxors. In this connection, it has already been argued that the lead ions play an essential rôle in promoting coupling between octahedral dipole moments in relaxors.[39]

Apart from these specific questions, the existence of a macroscopic rhombohedral symmetry in PMN at room temperature is of considerable significance. Until now, diffraction work on PMN has indicated macroscopic rhombohedral symmetry only when a high electric field is applied at low temperatures, whereas in the absence of a field at low temperatures, rhombohedral symmetry has been considered to exist merely within local microregions in a cubic matrix. Moreover, at room temperature the PMN crystallites are at a temperature above the Curie maximum. Although it has been speculated that compositional microregions could have local, polar rhombohedral symmetry characterised by a unique type of octahedral distortion,[22] macroscopic rhombohedral symmetry has, until now, been no more than a possibility requiring experimental verification.[40,41]

Also relevant is the finding that, in all the refinements, it was impossible to distinguish between Mg and Nb displacements. This implies that, despite these ions having different ionic radii, they both have similar off-centre shifts, $\Delta z_{Mg/Nb}$ (Table 4). Since, as previously argued, larger ions such as Mg^{2+} (and Zr^{4+} in $Pb(Mg_{1/3}Nb_{2/3})O_3$–$PbZrO_3$) promote rhombohedral symmetry, the relaxor properties of PMN are consistent with the notion that the MgO_6 octahedra are unable to give rise to large dipole moments. Conversely, the Nb^{5+} ions form large dipole moments, due to their high charges and relatively oversized oxygen octahedra. Thus, as has been proposed earlier,[37] a natural clustering into niobium-rich microregions can occur through the random occupation of B-sites by Nb^{5+} and Mg^{2+} ions. The results here suggest that the lattice itself is rhombohedral at temperatures up to 300 K, and not cubic, as is generally maintained.

5 Conclusion

Neutron diffraction studies have provided evidence for macroscopic rhombohedral symmetry in lead magnesium niobate at both 300 and 10 K.

Acknowledgements

The authors wish to thank the Swedish Royal Academy of Sciences for a special research grant to SAI. Thanks are also due to the DPST project and to the Thai Government for financial support of SA.

References

1. Smolenski, G. A. and Agranovskaya, A. I., Dielectric polarization and losses of some complex compounds. *Sov. Phys.-Tech. Phys.*, 1958, **3**, 1380–1382.
2. Cross, L. E., Relaxor ferroelectrics: an overview. *Ferroelectrics*, 1994, **151**, 305–320.
3. de Mathan, N., Husson, E., Calvarin, G., Gavarri, J. R., Hewat, A. W. and Morell, A., A structural model for the relaxor $PbMg_{1/3}Nb_{2/3}O_3$ at 5 K. *J. Phys.: Condens. Matter*, 1991, **3**, 8159–8171.
4. Husson, E., Chubb, M. and Morell, A., Superstructure in $PbMg_{1/3}Nb_{2/3}O_3$ ceramics revealed by high resolution electron microscopy. *Mater. Res. Bull.*, 1988, **23**, 357–361.
5. Chen, J., Chan, H. M. and Harmer, M. P., Ordering structure and dielectric properties of undoped and La/Na-doped $Pb(Mg_{1/3}Nb_{2/3})O_3$. *J. Am. Cer. Soc.*, 1989, **72**, 593–598.
6. Burns, G. and Dacol, F. H., The observation of glassy polarization behaviour in crystalline ferroelectric materials. *Ferroelectrics*, 1983, **52**, 103–113.
7. de Mathan, N., Husson, E. and Morell, A., Modification of the nanostructure and dielectric properties of lead magnoniobate ceramics by doping. *Mater. Res. Bull.*, 1992, **27**, 867–876.
8. Smolenskii, G. A., Physical phenomena in ferroelectrics with diffused phase transition. *J. Phys. Soc. Jpn. (Suppl.)*, 1970, **28**, 26–37.
9. Cross, L. E., Relaxor ferroelectrics. *Ferroelectrics*, 1987, **76**, 241–267.
10. Randall, C. A., Bhalla, A. S., Shrout, T. R. and Cross, L. E., Classification and consequences of complex lead perovskite ferroelectrics with regard to B-site cation order. *J. Mater. Res.*, 1990, **5**, 829–845.
11. Bonneau, P., Garnier, P., Calvarin, G., Husson, E., Gavarri, J. R., Hewat, A. W. and Morell, A., X-ray and neutron diffraction studies of the diffuse phase transition in $PbMg_{1/3}Nb_{2/3}O_3$ Ceramics. *J. Solid State Chem.*, 1991, **91**, 350–361.
12. Zhang, Q. M., You, H., Mulvilhill, M. L. and Jong, S. J., An X-ray diffraction study of superlattice ordering in lead magnesium niobate. *Solid State Comm.*, 1991, **97**, 693–698.
13. Verbaere, A., Piffard, Y., Yé, Z. G. and Husson, E., Lead magnoniobate crystal structure determination. *Mater. Res. Bull.*, 1992, **27**, 1227–1239.
14. Chen, I. W., Li, P. and Wang, Y., Structural origin of relaxor perovskites. *J. Phys. Chem. Solids*, 1996, **57**, 1525–1536.
15. Shebanov, L. A., Kapostins, P. P. and Zvirgzds, J., The structure change of PMN in the diffuse phase transition region. *Ferroelectrics*, 1984, **56**, 1057–1060.
16. Depero, L. E. and Sangaletti, L., Structural models for lead magnesium niobate. *Solid State Comm.*, 1997, **102**, 615–620.
17. Ye, Z. G., Relaxor ferroelectric $Pb(Mg_{1/3}Nb_{2/3})O_3$: properties and present understanding. *Ferroelectrics*, 1996, **184**, 193–208.
18. Chernyshev, V. V., Zhukov, S. G., Vakhrushev, S. B. and Schenk, H., Structural study of $Pb(Mg_{1/3}Nb_{2/3})O_3$ at low temperatures. *Ferroelectrics Letters*, 1997, **23**, 45–53.
19. Rosenfeld, H. D. and Egami, T., Short and intermediate range structural and chemical order in the relaxor ferroelectric lead magnesium niobate. *Ferroelectrics*, 1995, **164**, 133–141.
20. Egami, T., Teslic, S., Dmowski, W., Viehland, D. and Vakhrushev, V., Local atomic structure of relaxor ferroelectric solids determined by pulsed neutron and X-ray scattering. *Ferroelectrics*, 1997, **199**, 103–113.
21. Choi, S. W., Shrout, T. R., Jang, S. J. and Bhalla, A. S., Dielectric and pyroelectric properties in the $Pb(Mg_{1/3}Nb_{2/3})O_3$–$PbTiO_3$ system. *Ferroelectrics*, 1989, **100**, 29–38.
22. Tavernor, A. W. and Thomas, N. W., The dependence on chemical composition of the relaxor response of zirconium-substituted lead magnesium niobate ceramics. *J. Eur. Ceram. Soc.*, 1994, **13**, 121–127.
23. Ananta, S. and Thomas, N. W., A modified two-stage mixed oxide synthetic route to lead magnesium niobate and lead iron niobate. *J. Eur. Ceram. Soc.*, 1999, **19**, 155–163.
24. Rodrigues-Carvajal, J., Recent advances in magnetic structure determination by neutron powder diffraction. *Physica*, 1993, **B192**, 55–69.
25. Glazer, A. M. and Mabud, S. A., Powder profile refinement of lead zirconate titanate at several temperatures. *Acta Crystallogr.*, 1978, **B34**, 1065–1070.
26. Lehmann, A. G., Kubel, F., Ye, Z. G. and Schmid, H., Uniaxial birefringence in cubic $Pb(Fe_{0.5}Ta_{0.5})O_3$: is there a hidden symmetry-breaking? *Ferroelectrics*, 1995, **172**, 277–285.
27. Knight, K. S. and Baba-Kishi, K. Z., Crystal structure refinements of disordered $Pb(Sc_{0.5}Nb_{0.5})O_3$ in the paraelectric and ferroelectric states. *Ferroelectrics*, 1995, **173**, 341–349.
28. Husson, E., Abello, L. and Morell, A., Short range order in $PbMg_{1/3}Nb_{2/3}O_3$ ceramics by raman spectroscopy. *Mater. Res. Bull.*, 1990, **25**, 539–545.
29. Idink, H. and White, W. B., Raman spectroscopic study of order–disorder in lead magnesium niobate. *J. Appl. Phys.*, 1994, **76**, 1789–1793.
30. Arndt, H., Sauerbier, F., Schmidt, G. and Shebanov, L. A., Field-induced phase transition in $PbMg_{1/3}Nb_{2/3}O_3$ single crystals. *Ferroelectrics*, 1988, **79**, 145–148.
31. Calvarin, G., Husson, E. and Ye, Z. G., X-ray study of the electric field-induced phase transition in single crystal $Pb(Mg_{1/3}Nb_{2/3})O_3$. *Ferroelectrics*, 1995, **165**, 349–358.
32. Vakhrushev, S. B., Kiat, J. M. and Dkhil, B., X-ray study of the kinetics of field induced transition from the glass-like to the ferroelectric phase in lead magnoniobate. *Solid State Comm.*, 1997, **103**, 477–482.
33. Bidault, O., Licheron, M., Husson, E., Calvarin, G. and Morell, A., Experimental evidence for a spontaneous relaxor to ferroelectric phase transition in $PbMg_{1/3}Nb_{2/3}O_3$–10%Ti. *Solid State Comm.*, 1996, **98**, 765–769.
34. Thomas, N. W., Crystal structure-physical property relationships in perovskites. *Acta Crystallogr.*, 1989, **B45**, 337–344.
35. Thomas, N. W. and Beitollahi, A., The inter-relationship of octahedral geometry, polyhedral volume ratio and ferroelectric properties in rhombohedral perovskites. *Acta Crystallogr.*, 1994, **B50**, 549–560.
36. Thomas, N. W., A re-examination of the relationship between lattice strain, octahedral tilt angle and octahedral strain in rhombohedral perovskites. *Acta Crystallogr.*, 1996, **B52**, 954–960.
37. Thomas, N. W., A new global parameterization of perovskite crystal structures. *Acta Crystallogr.*, 1998, **B54**, 585–599.
38. Corker, D.L, Glazer, A. M., Whatmore, R. W., Stallard, A. and Fauth, F., A neutron diffraction investigation into the rhombohedral phases of the perovskite series, $PbZr_{1-x}Ti_xO_3$. *J. Phys.: Condens. Matter*, 1998, **10**, 6251–6269.
39. Thomas, N. W., A new framework for understanding relaxor ferroelectrics. *J. Phys. Chem. Solids*, 1990, **51**, 1419–1431.
40. Thomas, N. W., The influence of crystal chemistry on the ferroelectric and piezoelectric properties of perovskite ceramics. *Brit. Ceram. Procs.*, 1994, **52**, 1–12.
41. Thomas, N. W., Beyond the tolerance factor: harnessing X-ray and neutron diffraction data for the compositional design of perovskite ceramics. *Brit. Ceram. Trans.*, 1997, **96**, 7–15.